ELSEVIER

Journal of Hazardous Materials A79 (2000) 103–115

Journal of Hazardous Materials

www.elsevier.nl/locate/jhazmat

Sulphur condensation influence in Claus catalyst performance

Rafael Larraz Mora *

Chemical Engineering Department, University of La Laguna, Tenerife, Spain

Received 1 December 1999; received in revised form 25 February 2000; accepted 26 February 2000

Abstract

The Claus process is an efficient way of removing H_2S from acid gas streams and this is widely practised in industries such as natural gas processing, oil refining and metal smelting. Increasingly strict pollution control regulations require maximum sulphur recovery from the Claus unit in order to minimise sulphur-containing effluent. The most widely used Claus catalyst in sulphur recovery units is non-promoted spherical activated alumina. Properties associated with optimum non-promoted Claus catalyst performance include high surface area, appropriate pore size distribution and enhanced physical properties. The objective of this paper is to outline a procedure in order to estimate Claus catalyst effectiveness after pore plugging due to sulphur condensation. Catalyst deactivation due to pore plugging by sulphur is modelled employing a Bethe lattice and its corresponding performance is described by means of a modified effectiveness factor. Model results show an improvement in the modified effectiveness factor due to modifications in catalyst porous structure. © 2000 Elsevier Science B.V. All rights reserved.

Keywords: Hydrogen sulphide; Porous media modelling; Effectiveness factor; Catalyst deactivation; Sulphur production

1. Introduction

The modified Claus process is widely used to recover elemental sulphur from the hydrogen sulphide present in gases from oil refineries, natural gas, coal gasification and other industries. In the Claus reaction, hydrogen sulphide and sulphur dioxide react in

* Tel.: +34-922-602710; fax +34-922-218803.
E-mail address: rafael.larraz@tenerife.cepsa.es (R.L. Mora).

0304-3894/00/$ - see front matter © 2000 Elsevier Science B.V. All rights reserved.
PII: S0304-3894(00)00193-X

the vapour phase to produce sulphur and water. The two-step process can be described as:

$$3H_2S + 3/2O_2 = SO_2 + 2H_2S + H_2O$$

$$2H_2S + SO_2 = 3/nS_n + 2H_2O.$$

In the first step, one-third of the H_2S is oxidised in an oxigen deficienct atmosphere producing H_2S and SO_2 in a 2:1 ratio. Based on thermodynamics, conversion is about 70% at this stage and a second step with three to four catalytic stages is needed to obtain 95–98% conversion. The most widely used Claus catalyst in sulphur recovery units is non-promoted spherical activated alumina. Due to more strict environmental laws, Claus catalyst performance prediction is an important issue to assist refiners in catalyst selection and sulphur unit troubleshooting. One of the most common Claus catalyst deactivation mechanisms is pore plugging by means of sulphur capillary condensation. The S_1 through S_8 molecules formed via the modified Claus reaction can plug the catalyst pores at standard Claus converter conditions above the sulphur dew point. Increasing converter temperature avoids sulphur condensation but decreases Claus conversion that is favoured at low temperatures. The purpose of this paper is to outline a procedure in order to estimate Claus catalyst effectiveness after pore plugging due to sulphur condensation, and provide a method to improve catalyst performance. The catalyst is modelled as a Bethe lattice, and the model gives information about deactivation dynamics.

2. Sulphur capillary condensation

The elemental sulphur content of a used catalyst may be due to two-mechanisms: adsorption and condensation. The quantity of elemental sulphur adsorbed by the catalyst is a function of the catalyst temperature and the concentration of the sulphur in the gas phase. Typical steady state concentrations for first and second converters range between 3% and 10% by weight; for third and fourth converters the range is 10% to 15%. Adsorbed elemental sulphur is an unavoidable deactivating agent [1].

Elemental sulphur in a condensed form on the catalyst is also a severe deactivating agent. Plant operators circumvent this problem by operating the converter bed above the sulphur dew point. Unfortunately, sub dew-point operation often occurs as a result of poor condenser efficiencies, the lack of mist elimination devices after the condensers or faulty stream temperature measurements. Deactivation due to sub dew-point operation can usually be corrected by raising the converter temperature.

Sulphur capillary condensation in pores greater than 15 Å has been described [2] according to the Kelvin equation:

$$d = \frac{-4\gamma V \cos\theta}{RT \ln(p/p_0)} \tag{1}$$

where, d = pore diameter (cm); γ = liquid surface tension (dyn/cm); V = liquid molar volume (cm^3/mol); θ = contact angle (°); R = 8.314 E7 (erg/mol K); T = absolute

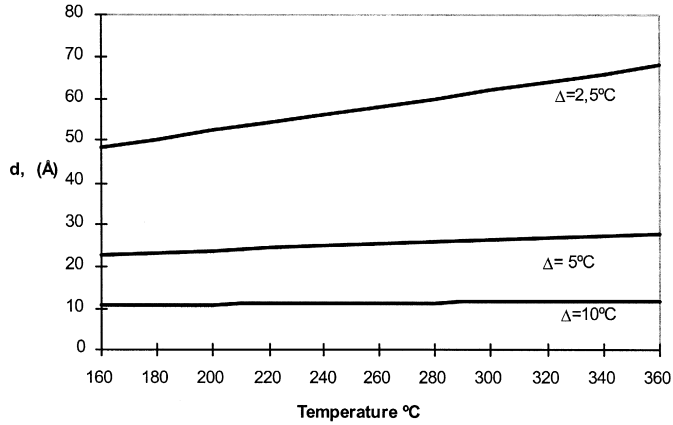

Fig. 1. Maximum pore diameter as a function of reactor temperature and dew-point safety margin.

temperature (K); p = vapour pressure of the condensing gas inside the pore (mm Hg); p_0 = vapour pressure of the condensing gas over a planar surface (mm Hg).

This equation clearly demonstrates that both the pore structure parameter, d, and the adsorbate–adsorbent interaction parameter $\gamma\cos\theta$, determine the capillary condensation. In the case of micropores $d < 10$ Å, the Kelvin equation does not apply because the pores are commensurate with the adsorbed molecules, which leads to a substantial increase in the adsorption energy as compared to the corresponding values for macro or meso porous adsorbents of a similar chemical nature.

Shoofs [2] applied the Kelvin equation modified by Cohan hypothesis, Eq. (2), on adsorption isotherm hysteresis, to sulphur condensation over alumina. The results presented in Fig. 1 show the maximum Claus catalyst pore diameters that will plug with sulphur as a function of catalyst converter temperature and the safety margin Δ, the difference between the catalytic converter temperature and the sulphur dew point temperature.

$$d = \frac{-2\gamma V}{RT\ln(p/p_0)}. \tag{2}$$

Claus unit operators following the recommendations of Fig. 1 usually set the safety margin Δ in excess of 10°C, thus decreasing Claus conversion in the reactors. From our point of view, sulphur condensation also affects the reaction rate and the catalyst surface area. Effectiveness factor accounts for these parameters and provides a feasible description for the sulphur condensation phenomena.

3. Claus reaction effectiveness factor

Catalysts are highly porous materials, and typically show some aspects of pore diffusion control. The effectiveness factor, η, for a catalyst is defined as the ratio of the

average reaction rate, r', divided by the rate at the catalyst surface, r. When the reaction rate presents constraints due to the porous structure of the catalyst pellet, the true reaction rate is given by:

$$r' = \eta r \text{ where } \eta = f(\phi) \tag{3}$$

and ϕ, the Thiele modulus, is the ratio of the reaction rate to the diffusion rate and is given by Weisz and Hicks [3].

$$\phi = R/3\left(r\,\rho_p/D_e C_c\right)^{1/2} \tag{4}$$

where R is the catalyst radius; ρ_p represents the pellet density; D_e is the effective diffusivity and C_c accounts for the reactant concentration. The effectiveness factor includes various potential rate-controlling factors such as the intrinsic catalytic reaction rate, both inter- and intra-particle mass and heat transfer rates, and the physical properties of the catalyst particles.

The effectiveness factor calculation for the Claus reaction involves considerable complexity due to the presence of multiple reaction steps in the system and the reversibility of the Claus reaction. The calculation of a local isothermal effectiveness factor depends upon the feed composition to the reactor, the extent of the conversion and the temperature at the exterior of the catalyst particle. Razzaghi and Dalla Lana [4] have proposed the use of a modified Thiele modulus, Φ, and a η vs. Φ curve applicable for the Claus reaction in the 500–600°K operating temperature range. The modified Thiele modulus has the form:

$$\Phi = \phi/\sqrt{(1 - \Psi_0)} \tag{5}$$

where $\Psi_o = p_{H_{2Seq}}/p_{H_2S}$ is included due to the thermodynamic equilibrium restriction inherent to the Claus reaction. The H_2S equilibrium partial pressure is calculated through the Gamson and Elkins [5] procedure. The η–Φ curve is presented in Fig. 2.

The effectiveness factor indicates the effect of pore structure influence on the catalyst performance. High values (> 0.90) indicates a rapid accessibility of the reactants to the

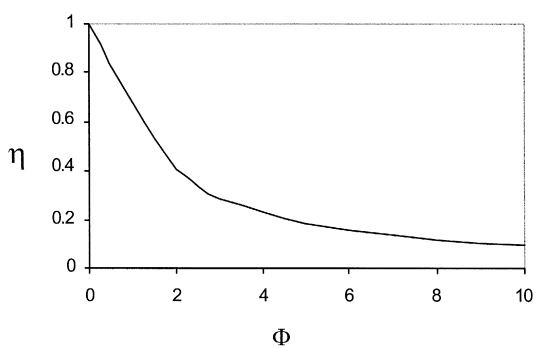

Fig. 2. η vs.Φ curve.

Table 1
Intrinsic rate expressions for Claus reaction

Author	Catalyst	k_0	E (J/mol)	b	n
McGregor et al. [29]	Bauxite	6.4E−3	31,149	0.0317	1
Dalla Lana et al. [8]	Alumina	5.24E−3	30,773	0.045	2
George [30][a]	Co–Mo alumina	–	23,500	–	1
Quet et al. [31]	Alumina	–	27,100		1
El Masry [32][b]	Alumina	–	35,100	0	–

$-r_{H_2S} = k_0 \mathrm{Exp}(-E/RT) p_{H_2S} p_{SO_2}^{0.5} / (1 + b p_{H_2O})^n$.
[a] Low activation energy due to diffusional limitations.
[b] Equation for optimisation procedure calculation.

active sites and products exit from the catalyst. Lower values means a lower catalyst efficiency and poor performance.

In calculating effectiveness factors for the Claus reaction system, the correct intrinsic rate function should be used. Table 1 lists several rate expressions and their authors. The similarity in form between equations independently obtained for different alumina-based catalysts suggests that the catalyst mechanism may be relatively insensitive to the physical structure of the alumina surface. Alternatively, this insensitivity to the catalyst surface could be a consequence of the presence of large amounts of sulphur being adsorbed on the surface [6,7]. Since during sulphur condensation the reverse reaction is not significant, it has been neglected. Sulphur condensation plugs catalyst pores and reduces surface area. A correction factor has been included in the rate equation to represent the activity loss due to catalyst surface area diminution [8], $E = S/S_0$; where S is the actual surface area and S_0 is the surface area from the catalyst tested to obtain the rate equation. This factor considers that catalyst activity is directly proportional to the number of accessible surface active sites. Surface area modifies Eq. (3) in the following form, accounting for the area reduction due to sulphur condensation phenomena:

$$r' = \eta E r \text{ and } \eta' = E\eta \tag{6}$$

where the intrinsic rate r, employed in the Thiele modulus calculation, is also affected by the term E, and a modified effectiveness factor, η', is introduced.

4. Representation of porous media and effective diffusivities

Mass transport inside catalytic porous particles has usually been described according the hypothesis of a pseudo-homogeneous media, where Fick's equation can be applied through an effective diffusivity, D_e:

$$N_i = -D_e \mathrm{d}C_i/\mathrm{d}r. \tag{7}$$

The effective diffusivity represents the heterogeneity of the catalyst particle in the microscopic scale and is usually defined as:

$$D_e = Df \tag{8}$$

where D is the average composite local diffusivity and f is a correction factor for taking into account the complex internal pore structure of the solid.

D, the average composite local diffusivity, is a function of the pore radius r if Knudsen diffusion is significant. Neglecting the composition effect and at constant pressure, D is given [9], for a pore radius r by:

$$1/D = 1/D_{AB} + 1/D_k \tag{9}$$

where D_{AB} is the bulk diffusivity for the binary gas mixture and D_k is the Knudsen diffusivity for A in a pore of radius r. The respective diffusivities are given by:

$$D_{AB} = 0.001853\, T^{3/2}\left(1/M_A + 1/M_B\right)^{1/2}/P_t \sigma_{AB}\, \Omega_{AB}\,; \text{bulk difussivity} \tag{10}$$

$$D_{k,\,\text{macro or micro}} = 9.7 \times 10^3\, r_{\text{macro or micro}}\left(T/M_A\right)^{1/2}; \text{Knudsen diffusivity}. \tag{11}$$

In the bulk regime, diffusion does not depend on pore size, and D is simply replaced by D_{AB}. In the Knudsen and transition regimes, the calculation of D requires that we include the contribution from pores of different sizes.

The pore structure of a catalyst pellet can be conveniently characterised by its pore size distribution determined by porosimetry. For bimodal pore structures, the relevant quantities are:

V_{macro}: macropore volume
V_{micro}: micropore volume
$r_{macro} = 1/V_{macro} \int r\mathrm{d}v$: macropore average radius
$r_{micro} = 1/V_{micro} \int r\mathrm{d}v$: micropore average radius
ρ_s: solid density.

Under the term micropores, we are considering pores smaller than 35 Å; macro and mesopores are those over 35 Å. Micro- and macropore average radius and volume are obtained this way. The following properties can be derived from:

$$\rho_p = 1/\left(1/\rho_s + V_{macro} + V_{micro}\right); \text{pellet density} \tag{12}$$

$$\varepsilon_{macro} = V_{macro}\, \rho_p; \text{macroporosity} \tag{13}$$

$$\varepsilon_{micro} = V_{micro}\, \rho_p; \text{microporosity}. \tag{14}$$

The surface area of the catalyst is directly related to its pore structure. For bimodal pore structures, as in alumina, integral properties allow a reasonably good correlation:

$$S = 2V_{macro}/r_{macro} + 2V_{micro}/r_{micro}\,. \tag{15}$$

Parameter f in Eq. (8) is a correction factor to account for the complex internal structure of the solid. Different levels of complexity have been used to describe the

orientation, size and interconnection of the pores. Among the models proposed in the literature, two groups can be distinguished:

- Capillary models
- Discrete models.

5. Capillary models

A capillary network ranging from a simple bundle of cylindrical capillaries [10] to a more complex random pore model [11] or a cross-linked pore model [12] with different geometry, are used as catalyst models. All these approaches take the parameter f in Eq. (8) as a tortuosity factor requiring matching the predictions to experimental data:

$$f = \varepsilon/\tau \tag{16}$$

where ε is the total porosity and τ the tortuosity. The tortuosity factor measures the increased diffusion path-length imposed by the presence of solid obstacles. It is therefore an intrinsic geometric property of the solid; it should be independent of the diffusion mechanism. In practice, however, tortuosity frequently becomes an adjustable parameter that compensates for inadequacies in evaluating the various terms of the defining Eq. (8). First, the equivalent diffusivity D does not take into account the connectivity of the pore space, also poorly inferred from adsorption or porosimetry data; cylindrical pore radii are used to describe the irregular shape of the pore cavities. Therefore, these approaches often lead to tortuosity values much greater than actual geometrical path-length and sensitive to temperature and pressure [13]. Capillary models are not well suited for describing drastic changes in catalyst connectivity and underlying phenomena like pore plugging due to sulphur condensation.

6. Discrete models

Discrete models are free of capillary model limitations but require a higher computational effort. These models consider that the catalyst is sufficiently disordered that a statistical description matches its connectivity and associated transport properties. Percolation theory [14] has been widely applied to describe a porous matrix and associated transport properties [15].

In the terminology of percolation processes, the medium is defined as an infinite set of objects called sites. For porous media applications, sites are equivalent to pore bodies where pore throats join each other. A fluid introduced at a site, called a source site, flows along various path connection sites, called bonds which are essentially pore throats. The number of bonds connected to a site is called its coordination number, Z. Two sites are called connected if there exists at least one path between them consisting only of occupied bonds. A set of connected sites bounded by vacant bonds is called a cluster. A lattice characteristic parameter is the percolation threshold, ε^{c}, which is the largest fraction of occupied bonds below which there is no sample spanning cluster of

occupied bonds. The derivation of exact characteristic values for discrete models has been possible to date only for certain lattices related to the Bethe lattice and for a few two-dimensional lattices.

7. Bethe lattice model

A Bethe lattice is a branching structure with no closed loops. Bethe networks have been widely used as models of pore space topology [16–19], and in catalyst deactivation analysis [20].

In percolation theory, the accessible porosity, ε^{A}, is defined as the likelihood that any pore region is sufficiently well connected to the rest of those available for transport, and total porosity, ε, is the sum of the accessible porosity and porosity in isolated pores, ε^{I}. Evaluation of ε^{A}, ε^{I}, ε and parameter f from Eq. (8) [21] can be evaluated by employing the Bethe lattice as a model of pore space topology.

Percolation threshold is calculated [22] as:

$$\varepsilon^{c} = 1/(Z-1) \tag{17}$$

the values of accessible, ε^{A}, and isolated porosity, ε^{I}, are given by:

$$\begin{array}{ll} 0 & \text{for } \varepsilon < p_{cs} \\ \varepsilon\left(1-\left(\varepsilon^{R}/\varepsilon\right)^{(2Z-2)/(Z-2)}\right) & \text{for } \varepsilon > \varepsilon^{c} \end{array} \tag{18}$$

with:

$$\begin{aligned} &\varepsilon^{R}\left(1-\varepsilon^{R}\right)^{(Z-2)} - \varepsilon\left(1-\varepsilon\right)^{(Z-2)} = 0 \\ &\varepsilon^{I} = \varepsilon - \varepsilon^{A} \end{aligned} \tag{19}$$

If the porosity value is close to ε^{c}, then parameter f can be obtained by:

$$f = 1.522\left(\varepsilon-\varepsilon^{c}\right)^{2}\left(Z-1\right)^{3}/\left(Z-2\right)^{2}. \tag{20}$$

When porosity is far from percolation threshold parameter, f takes the following form:

$$f = (Z-1)/(Z-2)\sum G_{s} \tag{21}$$

$(s = 0, \ldots 3)$ where:

$$\begin{aligned} G_{0} &= -\left(\varepsilon-\varepsilon^{c}\right) \\ G_{1} &= 0 \\ G_{2} &= \left(\varepsilon^{c}/\varepsilon\right)^{2}\left(\varepsilon-\varepsilon^{c}\right)(1-\varepsilon) \\ G_{3} &= \left(\varepsilon^{c3}/\varepsilon^{5}\right)\left(\varepsilon-\varepsilon^{c}\right)(1-\varepsilon)\left[\varepsilon(2\varepsilon-1)+2\left(\varepsilon-\varepsilon^{c}\right)(1-\varepsilon)\right] \end{aligned} \tag{22}$$

Table 2
Alumina physical properties

Parameter	Alumina
ρ_s (g/cm^3)	3.15
ρ_p (g/cm^3)	1.27
V_{macro} (cm^3/g)	0.117
V_{micro} (cm^3/g)	0.348
r_{macro} (Å)	7589
r_{micro} (Å)	20
ε_M	0.15
ε_m	0.44
S (m^2/g)	353
d ($''$)	1/4

As alumina presents a bimodal pore structure, two effective diffusivites can be considered, one for the micropores, D_{em}, and D_{eM} for the meso-macropore. The global effective diffusivity is obtained by means of:

$$D_e = D_m f_m + D_M f_M . \quad (23)$$

Discrete models such as Bethe lattice, seem to have the advantage of a constant Z with porosity changes [23,24], and thus are suitable for catalyst dynamics description of sulphur pore plugging conditions.

8. Calculation procedure and results

In the calculations, a typical alumina Claus catalyst has been employed using the physical parameters presented in Table 2. Typical Claus unit operation conditions have been considered and are presented in Table 3. Catalyst performance under sulphur condensation conditions is given by Eq. (6). In order to simulate the modification of the catalyst due to sulphur plugging, the micropore volume has been reduced in 0.05 ml/g intervals. Textural parameters such as surface area, porosity and average micropore radius are calculated using Eqs. (12)–(15), and the effective diffusivity is obtained employing the Bethe lattice model. The alumina coordination number has been determined from porosimetry analysis to be between 5 and 6 [25]. Since $Z = 6$ matches

Table 3
Catalytic converters operation conditions

Parameter	Reactor 2	Reactor 3
Temperature (°C)	275	220
vol.% H_2S	2	1
GHSV (h^{-1})	500	500

Atmospheric operating pressure.

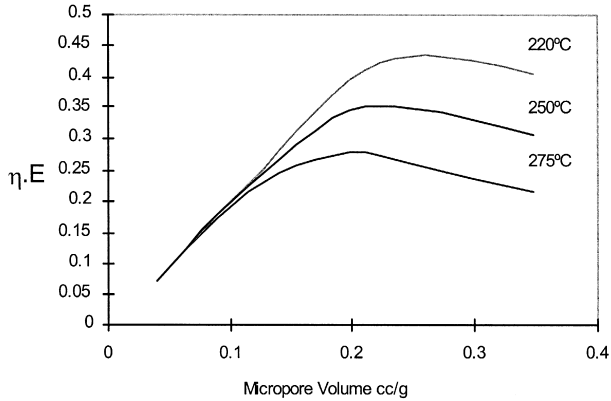

Fig. 3. Modified effectiveness factor vs. micropore volume.

experimental measurements [26], this value has been used. Effective diffusivity along with factor E and reaction rate (Table 1) provides the modified effectiveness factor for each micropore volume.

The sensitivity analysis of the modified effectiveness factor to model parameters is presented in Figs. 3–5. The modified effectiveness factor is represented as a function of micropore volume and pore radius at three different reactor temperatures and for reactant concentrations characteristic of a second and a third Claus reactor stages. Fig. 6 illustrates the variation of the effectiveness factor and surface area as the pore radius is varied.

A new insight is obtained from Figs. 3–5. When sulphur condenses into the pores, two opposite phenomena coexist. Low reaction rates and surface area reduction cause an increase in the effectiveness factor, which improves the modified effectiveness factor

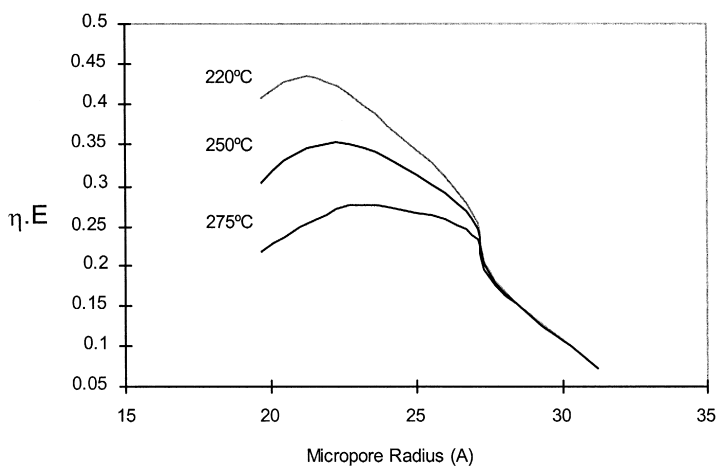

Fig. 4. Modified effectiveness factor vs. micropore radius.

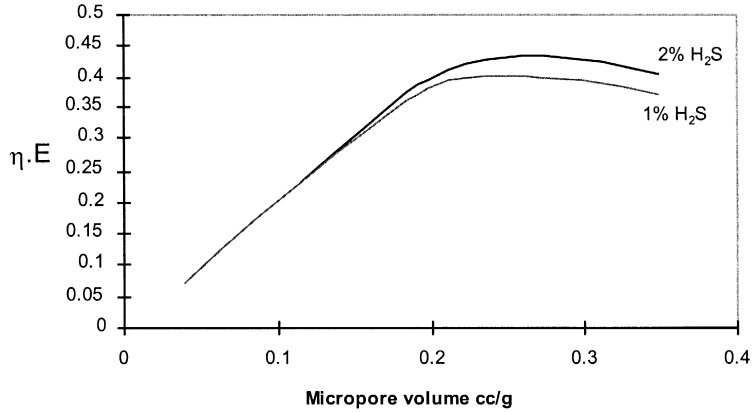

Fig. 5. Modified effectiveness factor vs. micropore volume for two different reactant concentrations.

allowing an improvement in the catalyst performance. The extent of this behaviour depends on the pore size distribution of each catalyst and on the operating conditions. For the catalyst examined, a micropore volume of 0.22 ml/g results in optimum performance, but performance decreases sharply as micropore volume is further reduced. Reactor temperature, as shown in Fig. 3, improves the effectiveness factor, but the behaviour under micropore volume diminution is essentially the same. From Fig. 4 we can see that for the catalyst under study this phenomenon is limited to pores sizes 15 to 25 Å; for pores larger than 25 Å a sharp reduction in catalyst performance is observed. According to the Shoofs model, these pore sizes correspond, as shown in Fig. 1, to a safety margin around 4°C to 6°C from the dew-point. Operating temperatures in this range could lead to significant improvements in Claus conversion as has been confirmed by operating data [27]. The increase in the modified effectiveness factor persists at different H_2S reactant concentrations as shown in Fig. 5.

Fig. 6 presents the effectiveness factor, according to Eq. (3), and the surface area variation with the micropore volume for a reactor temperature of 275°C. The opposite effects are presented as separated curves to show that, at certain micropore volumes

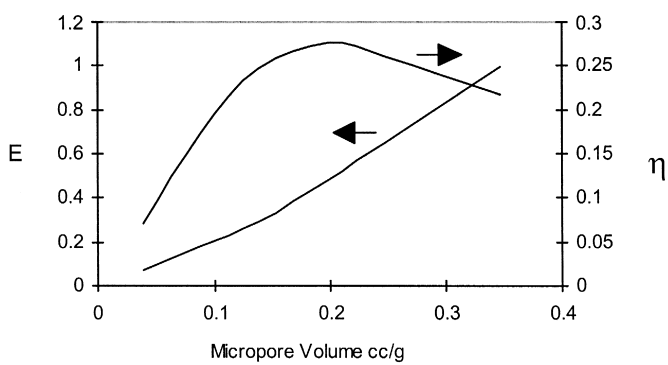

Fig. 6. Effectiveness and area variation vs. micropore volume for 275°C reactor temperature.

under sulphur condensation conditions, a threshold phenomena is present that allows for better conversions than expected.

Figs. 3–5 are characteristic for each different catalyst due to its dependence on the pore size distribution. Modern catalysts with less micropores and more macropores [28] are well suited for operating conditions as described, keeping reactor temperatures closer to the sulphur dewpoint and allowing higher unit conversion.

9. Conclusions

Claus catalyst deactivation due to sulphur condensation has been studied employing a mathematical model based on effectiveness factor calculation and a Bethe lattice as catalyst model. Results show an improvement in catalyst performance under deactivation conditions due to an increase of the modified effectiveness factor, which accounts for pore volume modifications due to sulphur condensation. This behaviour allows reactor temperatures closer to the sulphur dewpoint, improving the plant performance.

10. Nomenclature

b	Adsorption term in rate equations of Table 1
C_c	Reactant concentration (Units as a function of rate equation)
D_A	Bulk diffusivity (cm^2/s)
D_{eff}	Effective diffusivity (cm^2/s)
D_k	Knudsen diffusivity (cm^2/s)
D	Combined diffusivity (cm^2/s)
E	Surface area factor
f	Structural correction factor Eq. (8)
M_{AoB}	Molecular weight
N_i	Mass flux ($kmol/m^2$ s)
p_{H_2S}	H_2S partial pressure (atm)
$P_{H_{2Seq}}$	H_2S equilibrium partial pressure (atm)
P	Total pressure (atm)
R	Catalyst diameter (cm)
$r_{macro\ or\ micro}$	Macro or micropore radius (Å)
r	Catalyst surface reaction rate
r'	Average reaction rate
S	Surface area (m^2/g)
S_0	Original surface area (m^2/g)
T	Temperature (K or °C)
$V_{macro\ or\ micro}$	Macro or micropore volume (cm^3/g)
Z	Coordination number
Greek Letters	
ε	Total porosity
ε^A	Accesible porosity

ε^{c}	Percolation threshold
ε^{I}	Isolated porosity
ε^{R}	Root in Eq. (19)
ε	Porosity
η	Effectiveness factor
η'	Modified effectiveness factor, Eq. (6)
ϕ	Thiele modulus
Φ	Modified Thiele modulus
Ψ_0	Factor as defined in Eq. (3)
$\rho_{s \text{ or } p}$	Solid or pellet density
σ	Lennard–Jones constants
Ω	Collision integral, unity if molecules are considered rigid spheres
τ	Tortuosity factor

References

[1] R. Kerr, H.G. Paskall, N. Ballash, Energ. Proc. Can. 46 (1977) 40–51.
[2] G.R. Schoofs, Hydrocarbon Process. (1985) 71–73, February.
[3] P.B. Weisz, J.S. Hicks, Chem. Eng. Sci. 17 (1962) 265.
[4] M. Razzaghi, I.V. Dalla Lana, Can. J. Chem. Eng. 62 (1984) 413.
[5] B.W. Gamson, R.H. Elkins, Chem. Eng. Prog. 49 (4) (1953) 203.
[6] M. Steinjs, P. Mars, Ind. Chem. Prod. Res. Dev. 16 (1) (1977) 35.
[7] S. Mendioroz, V. Muñoz, E. Alvarez, J.M. Palacios, Appl. Catal., A 132 (1995) 111.
[8] I.G. Dalla Lana, C.L. Liu, B.K. Cho, 4° Int. Symp. Chem. React. Eng. (1976) V-196–V-205, Frankfurt.
[9] R.B. Evans, J. Truitt, G.M. Watson, J. Chem. Phys. 72 (1961) 2967.
[10] A. Wheeler, Adv. Catal. 3 (1951) 237.
[11] N. Wakao, J.M. Smith, Chem. Eng. Sci. 17 (1962) 825.
[12] M.F.L. Johnson, W.E. Stewart, J. Catal. 4 (1965) 248.
[13] S. Reyes, K.F. Jensen, Chem. Eng. Sci. 40 (1985) 1723.
[14] J.W. Broadbant, J.M. Hammersley, Proc. Cambridge Philos. Soc. 53 (1957) 629.
[15] M. Sahimi, G.R. Gavalas, T.T. Tsotsis, Chem. Eng. Sci. 45 (1990) 1443.
[16] A. Santos, A. Bahamonde, P. Avila, F. Garcia Ochoa, Appl. Catal., B 8 (1996) 299.
[17] F. Garcia Ochoa, A. Santos, AIChE J. 42 (1996) 2.
[18] S. Reyes, E. Iglesi, J. Catal. 129 (1991) 457.
[19] R.G. Larson, L.E. Scriven, H.T. Davis, Chem. Eng. Sci. 36 (1981) 57.
[20] G.F. Froment, NATO Adv. Study Inst. Ser., E 54 (1982) 103.
[21] R.B. Stimchombe, J. Phys. Chem. Solid State Phys. 7 (1974) 179.
[22] M.E. Fisher, J.W. Essam, J. Math. Phys. 2 (1961) 609.
[23] S. Reyes, K.F. Jensen, Chem. Eng. Sci. 41 (1986) 333.
[24] S. Reyes, K.F. Jensen, Chem. Eng. Sci. 41 (1986) 345.
[25] N.A. Seaton, Chem. Eng. Sci. 46 (8) (1991) 1895.
[26] C. Wang, J.M. Smith, AIChE J. 29 (1983) 1.
[27] J.A. Sames, Proc. Sulphur Recovery Seminar vol. 5, 1995, pp. 1–13, Estambul.
[28] R. Larraz, Hydrocarbon Process. (1999) 69–72, July.
[29] D.E. McGregor, I.G. Dalla Lana, C.L. Liu, E. Cormode, Proc 4th Europe/2nd Int. Symp. Chem. Eng. Reaction Eng., Elsevier, 1972, pp. 9–18.
[30] Z.M. George, J. Catal. 32 (1974) 261.
[31] C. Quet, J. Tellier, R. Voirin, Catal. Deact. 56 (1980) 323.
[32] H.A. El Masry, Appl. Catal. 16 (1985) 301.